Punctured Trellis-Coded Modulation

Fabian Schuh, Andreas Schenk, and Johannes B. Huber
Institute for Information Transmission, Friedrich-Alexander-Universität Erlangen-Nürnberg, Germany
mail: {schuh, schenk, huber}@LNT.de

***Abstract*—THIS PAPER IS ELIGIBLE FOR THE STUDENT PAPER AWARD**

In classic trellis-coded modulation (TCM) signal constellations of twice the cardinality are applied when compared to an uncoded transmission enabling transmission of one bit of redundancy per PAM-symbol, *i.e.*, rates of $\frac{K}{K+1}$ when 2^{K+1} denotes the cardinality of the signal constellation. In order to support different rates, multi-dimensional (*i.e.*, $\mathcal{D}$-dimensional) constellations had been proposed by means of combining subsequent one- or two-dimensional modulation steps, resulting in TCM-schemes with $\frac{1}{\mathcal{D}}$ bit redundancy per real dimension. In contrast, in this paper we propose to perform rate adjustment for TCM by means of puncturing the convolutional code (CC) on which a TCM-scheme is based on. It is shown, that due to the nontrivial mapping of the output symbols of the CC to signal points in the case of puncturing, a modification of the corresponding Viterbi-decoder algorithm and an optimization of the CC and the puncturing scheme are necessary.

***Index Terms*—trellis-coded modulation (TCM); multi-dimensional and pragmatic TCM; punctured convolutional codes; Viterbi-Algorithm (VA);**

I. Introduction

Ungerboeck's trellis-coded modulation (TCM) [1], [2] is an attractive digital transmission scheme when low over-all delay is desired. Low latency is ensured by the use of convolutional codes instead of block codes (*cf.* [3]) and the dispense with interleaving (as opposed to convolutional bit-interleaved coded modulation [4]).

Ungerboeck showed that a significant increase in Asymptotic Coding Gain (ACG) can be achieved when considering channel coding and modulation jointly. By expanding the constellation from 2^K to 2^{K+1} signal points and employing a rate-$\frac{K}{K+1}$ convolutional encoder one can improve the noise robustness of the transmission by upto 6 dB without any further costs besides computational effort [1]. High transmission rates can be achieved when additional uncoded bits are used to address the signal points. The most important modification to Ungerboeck's TCM propbably is the extension to multiple dimensions [5] accommodating non-integer transmission rates by grouping consecutive modulation symbols and constructing a $\mathcal{D}$-dimensional signal space.

Alternatively, in this paper, puncturing the channel code from a mother code is considered. As already described in [6], [7], in this case metric computations become time-dependent, as does the trellis diagram. In contrast to the modified metric increment suggested in [7], we propose Maximum-Likelihood (ML) decoding using a modified Viterbi algorithm (VA). Thus our approach enables ML-decoding of pragmatic punctured TCM for arbitrary rates. We performed extensive computer simulations in order to optimization the CC and the puncturing scheme.

This approach can be extended to ISI-channel scenarios. In this case, ML-decoding can be performed using the matched decoding scheme of [8], [9].

This paper is structured as follows: First, we briefly introduce notation and the system model in consideration in Sec. II. Sec. III recapitulates TCM and introduces a presentation technique that enables the implementation of punctured encoding in Sec. IV. A code search has been performed to find the best codes for out purpose in Sec. V. Final results and conclusions are given in Sec. VI and Sec. VII, respectively.

II. System Model

This paper deals with convolutionally encoded pulse-amplitude modulated (PAM) transmission[1] as depicted in Fig. 1. A binary data sequence $\langle u \rangle$ is split into n_u parallel

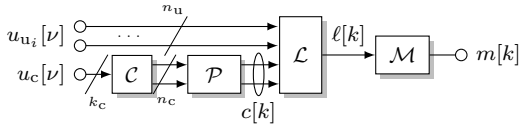

Fig. 1. System model for punctured trellis-coded modulation (P-TCM).

uncoded sequences $u_\mathrm{u}[\nu]$ and k_c parallel sequences $u_\mathrm{c}[\nu]$ that are encoded using a rate-$\frac{k_\mathrm{c}}{n_\mathrm{c}}$ binary convolutional $\mathcal{C}$ encoder with generator polynomials $[\, g_{ij} \,]\,,\ 1 \le i \le n_\mathrm{c}; 1 \le j \le k_\mathrm{c}$, with k_c parallel input symbols and n_c parallel output symbols at each time instant. At each output of the encoder, the symbols traverse through a puncturing system with puncturing scheme $P = [P_{ij}] \in \{0, 1\}\,;\ 1 < i \le n_\mathrm{c};\ 1 < j < \Omega$ and period Ω. For each encoder input symbol the puncturing scheme cyclically advances by one step. Where P_{ij} is zero, the current symbol at the output is discarded, accordingly. The punctured n_c-ary encoded output symbols $c[k]$ together with the uncoded input symbols $u_\mathrm{u}[\nu]$ are labeled to $\ell[k]$ before being mapped to the $M = 2^{n_\mathrm{u}+n_\mathrm{c}}$-ary signal constellation.

Throughout this paper we will use the following notation:

- $u[\nu] \in \{0,\, 1\}$ is the binary input sequence for the encoder at time instant ν

This work was supported by Federal Ministry of Economics and Technology (BMWi) within the project C-PMSE.

[1]here, the term PAM is used for complex-valued signal constellations as well including amplitude-shift keying (ASK), phase-shift keying (PSK) or quadrature-amplitude modulation (QAM)

- $c[k] \in \{0, 1\}$ denotes the encoded (possibly punctured) symbol
- $\ell[k] \in \mathcal{L}$ denotes the signal number from the set of labelings $\mathcal{L}$ (*e.g.*, natural labeling)
- $m[k] \in \mathcal{M}$ is the modulated symbol (*e.g.*, bipolar ASK). $\mathcal{M}$ denotes the modulation alphabet of size $M = |\mathcal{M}|$
- $P = [P_{ij}] \in \mathcal{P}$ denotes the puncturing scheme

The overall transmission rate of this scheme is $R = R_\mathrm{c} R_\mathrm{p} n_\mathrm{c} + n_\mathrm{u}$ with $R_\mathrm{c} = \frac{k_\mathrm{c}}{n_\mathrm{c}}$ and R_p being the rate of the channel encoding and puncturing, respectively. The rate of the puncturing can be calculate from the puncturing scheme by:

$$R_\mathrm{p} = \frac{n_\mathrm{c}\Omega}{\sum_i \sum_j P_{ij}}. \tag{1}$$

III. Trellis-Coded Modulation

In order to introduce maximum-likelihood sequence estimation (MLSE) for punctured TCM, we first briefly recall the encoding and mapping process for *non-punctured* TCM and introduce a representation for the encoding process and the state transitions of the finite-state-machine (FSM) (*cf.*, [2]).

A. System Model

In the case of TCM, the number of output symbols from a rate-$\frac{k_\mathrm{c}}{n_\mathrm{c}}$ encoder is related to the size of the modulation alphabet M so that $n_\mathrm{c} = \log_2(M)$ and $k_\mathrm{c} = n_\mathrm{c} - 1$ holds.

Fig. 2 shows an example of such a TCM transmitter with $n_\mathrm{u} = 0$, $k_\mathrm{c} = 1$ and a rate-$\frac{1}{2}$ encoder. Obviously, one of the two channel encoder output symbols (before puncturing) contains redundancy only.

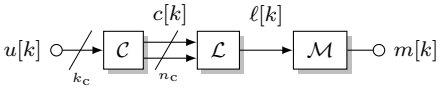

Fig. 2. Concatenation of a rate-$\frac{1}{2}$ convolutional encoder $\mathcal{C}$, a labeling and modulation. No puncturing is applied ($k_\mathrm{u} = 0$, $k_\mathrm{c} = 1$, $n_\mathrm{c} = 2$).

The coded bits are mapped onto a single transmit symbol $m[k]$ out of a modulation alphabet of size 2^{n_c}. Thus, after labeling and modulation, the overall transmission rate of TCM is $R = k_\mathrm{c} + n_\mathrm{u}$. The decoding trellis is well-known, time-invariant and has 2^{k_c} state transitions for each state.

In the following we describe the encoding process and the FSM to span a trellis. For simplicity of explanation, we focus on a rate-$\frac{1}{2}$ encoder and 4-ary modulation. We restrict ourselfs to nonrecursive encoding [1].

Fig. 3 illustrates the encoding process. The uncoded unipolar information sequence $u[k] \in \{0, 1\}$ is inserted into the FSM as input values and later passes through all delay elements describing the state of the FSM. Here, the generator polynomials g_1 and g_2 process the input symbol together with the FSM state synchronously at each time instant. The resulting encoded bits, denoted by MSB and LSB, respectively, are labeled into $\ell[k]$ and modulated in $m[k]$ to the 4-ary symbol alphabet of the transmission scheme, *e.g.*, via $m[k] = 2(2\mathrm{MSB} + \mathrm{LSB}) - 1$ for natural labeling and bipolar ASK (*cf.*, Sec III-B).

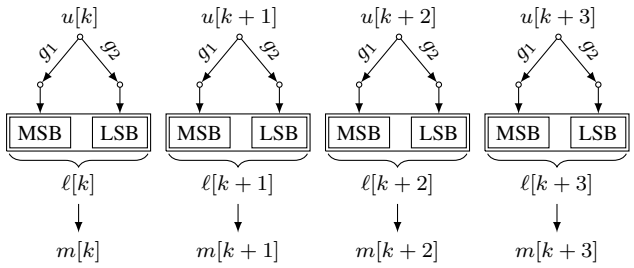

Fig. 3. Encoding process for a rate-$\frac{1}{2}$ convolutional code and 4-ary natural mapping. Overall transmission rate $R = 1$.

Fig. 4 depicts the state transitions of the FSM, when no puncturing is involved. The states are represented as memory elements in a first-in first-out (FIFO) register. The time-invariance of the trellis becomes clear, as each input symbol passes the same encoding procedure with g_1 and g_2, and labeling and modulation are independent of the time instant. As we will see later, this statement does not hold for punctured coding. We use the following representation:

- dark gray blocks (■) declare the trellis state
- light gray blocks (□) define the input values to the FSM and thus, the state transitions
- bars ($\overset{g_1}{\vdash\!\!\dashv}$) describe an arbitrary generator polynomials in binary representation

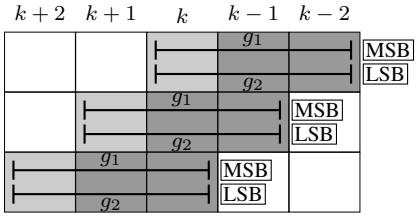

Fig. 4. State transitions of the transmitter FSM and the relations between generator polynomials and FSM-state/input with $\nu = 2$.

B. Labelings and Modulation

Labeling and modulation can either be implemented using a lookup table for $\mathcal{L}$ and $\mathcal{M}$, or via analytical formulas.

E.g., for the 4-ary natural labeling we multiply the MSB by 2 and add the LSB, *i.e.*, $\ell[k] = 2\mathrm{MSB}[k] + \mathrm{LSB}[k]$. An implementation of an ASK modulator can be seen as unipolar binary symbols $\ell[k]$, mapped onto bipolar symbols $m[k]$ within an alphabet of size M with $m[k] = (\ell[k] \cdot 2) - (M - 1)$.

Different labelings are easily incorporated, *e.g.*, a Gray labeling can be achieved by $\ell[k] = (1 - \mathrm{MSB}[k])(2\mathrm{MSB}[k] + \mathrm{LSB}[k]) + (\mathrm{MSB}[k])(2\mathrm{MSB}[k] + (1 - \mathrm{LSB}[k]))$.

C. Trellis-based Decoding

In the following section we will briefly describe the application of a trellis-based decoding algorithm for Ungerboeck's TCM. The trellis encoder of the transmitter can be used to generate the hypothesis and the state transitions of a FSM. The full-state receiver for a non-punctured coding is depicted in Fig. 5 and uses the hypothesis to calculate the metrics $\lambda_i[k]$, *e.g.*, squared Euclidean distances between the received signal and the hypothesis, for the noisy received signal. The

trellis-based decoding algorithm, such as the VA, estimates the transmitted data sequence by the use of the trellis and the metrics.

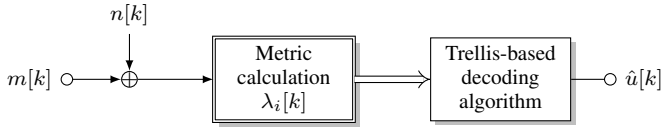

Fig. 5. The full-state trellis-based decoding, *e.g.*, with the VA.

IV. Punctured Trellis-Coded Modulation

In the following, we will describe the necessary modifications when punctured coding is applied.

A. System Model

A system model of punctured convolutional coding, without transmission of uncoded bits, *i.e.*, $n_\mathrm{u} = 0$, is depicted in Fig. 6.

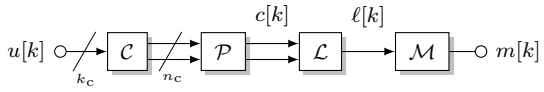

Fig. 6. Concatenation of a rate-$\frac{1}{2}$ convolutional encoder $\mathcal{C}$ and puncturing $\mathcal{P}$ with labeling and modulation ($k_\mathrm{u} = 0$, $k_\mathrm{c} = 1$, $n_\mathrm{c} = 2$).

By coded modulation with puncturing, we can achieve a transmission rate of $R = R_\mathrm{c} R_\mathrm{p} R_\mathrm{m}$. For reasons we will see later, our approach is constraint to $n_\mathrm{c} = 2$, *i.e.*, $R_\mathrm{c} = \frac{1}{2}$. Hence, the transmission rate is only determined by $R_\mathrm{p} \in [\,1, 2\,[$. Note that in the latter, the *mother code* defines the size of the modulation alphabet while the rate is increased by puncturing.

In the following, we exemplarily focus on $k_\mathrm{u} = 0$, $k_\mathrm{c} = 1$, $n_\mathrm{c} = 2$ and the puncturing scheme $[\,1\,1;\,0\,1\,]$.

First, we describe the encoding process and state transitions when *punctured* codes are used, and discuss the FSM for punctured convolutional codes as well as the modifications necessary for the VA to run in the resulting trellis.

When *punctured* convolutional codes are used, the relation that one uncoded information bit results in one modulation symbol is not valid any longer. Note that, whenever the number of erased bits in one period of the puncturing scheme is not devideable by $\log_2(M)$, the puncturing scheme has to be repeated until this condition is fulfilled. This restriction ensures that entire modulation symbols can be constructed by the FSM. In our case, the puncturing period (*e.g.*, $[\,1\,1;\,0\,1\,]$) is applied twice. As can be seen from the encoding procress in Fig. 7, the third and the seventh encoded symbol is punctured and does not contribute to the labeling and mapping process. The transitions of the FSM, depicted in Fig. 8, show two differences when compared to *non-punctured* FSM transitions (*cf.*, Fig. 4). These are described subsequently.

1) Generator Offsets $\mathcal{T}_i$: It becomes clear that the strict relations between the MSB, LSB and the generator polynomial g_1 and g_2, respectively, no longer hold. The second symbol, *i.e.*, $m[\nu+1]$, contains information about $u[\nu+1]$ and $u[\nu+2]$. In addition, the MSB is now generated by g_2 instead of g_1. Accordingly, the LSB, which was generated by g_2 in the *non-punctured* case, is now generated by g_1. It is also clear that the third symbol is generated by $u[\nu+2]$ and $u[\nu+3]$ using the generator polynomial g_2 twice.

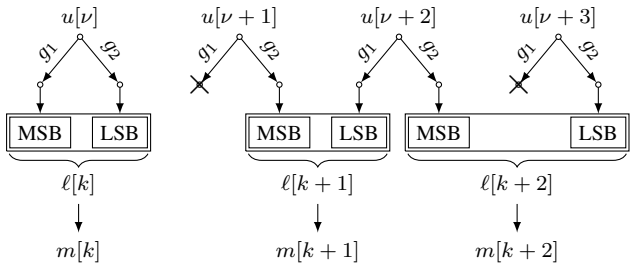

Fig. 7. Encoding process for a rate-$\frac{2}{3}$ punctured convolutional code and natural labeling. Overall transmission rate $R = \frac{4}{3}$.

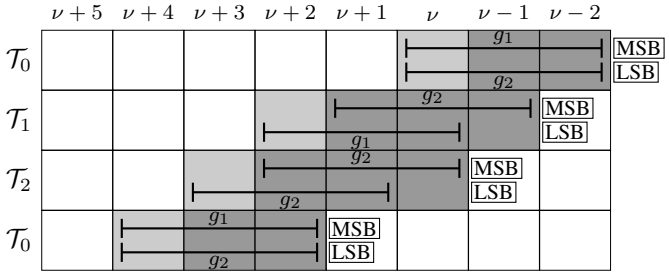

Fig. 8. State transitions of the transmitter FSM and the relations between generator polynomials and FSM-state/input.

To handle these relations we introduce a set of so called generator offsets $\mathcal{T}_i$ which describe, depending on the puncturing scheme, modulation size and time instant, the relations between generator polynomials, input value, FSM state, and mapping to MSB or LSB, respectively.

In our example, $\mathcal{T}_1$ indicates that the MSB output symbol can be determined by the memory (■) only, regardless of the current input symbol. On the other hand, in order to calculate the LSB we have to use the input value (■) and g_1. Obviously, the information in the LSB is one step ahead of the MSB. Thus, we need to extend the trellis at this point and can calculate the MSB using the FSM state and the generator polynomial g_2. Note that in case of $M = 4$, $\mathcal{T}_0$ indicates that no puncturing is active, *i.e.*, an even number of puncturings occurred up to time instant ν, and the generator polynomials are synchronized with LSB and MSB. $\mathcal{T}_1$ is used, whenever an odd number of puncturings has happened and $\mathcal{T}_2$ is used when the next puncturing synchronize the generator polynomials with MSB and LSB again. The number of generator offsets needed to describe all steps depends on the size of the modulation alphabet, whereas the generator offsets depend also on the puncturing scheme.

2) State Extension: The FSM transitions in Fig. 8 show that the symbol $m[\nu+1]$ contains information on the uncoded information bits $u[\nu+1]$, for which the MSB output was punctured, and the consecutive information bit $u[\nu+2]$. We see that, when generating the output, the calculation of the LSB is one step ahead to the MSB and considers one extra information bit. This results in a trellis that has to be expanded (*i.e.*, splitted) by a factor of two. This can be easily seen from Fig. 8 as the generator polynomials in the second step (generator offsets $\mathcal{T}_1$) now cover four blocks instead of just three. However, for a 4-ary transmission, when puncturing is

performed a second time, MSB and LSB are resynchronized with the generator polynomials and a so called *merge* happens in the trellis.

When considering $M > 4$, a resynchronization will appear after $\log_2(M)$ punctured bits. Extending the FSM to handle $n_\mathrm{c} > 2$ does not seem to be a good alternative choice, due to an increasing number of generator offsets and the significant increase of computational complexity. Hence, we restrict ourselves to $n_\mathrm{c} = 2$ for complexity reasons.

Therefore, a trellis based decoding algorithm, such as the VA, has to be performed on a time-variant trellis diagram. An example trellis for a punctured convolutional code with a constraint length $\nu = 2$ will be given below.

B. Trellis-based Decoding

In the following we will exemplarily describe trellis-based decoding for punctured convolutional codes.

When using the puncturing scheme $[\,1\,0;\,1\,1\,]$ introduced above the VA has to estimate four bits within three symbols from the trellis transitions. In order to see the modifications of the VA we need to consider the state extension.

Using Fig. 8, we define in each step $\mathcal{T}_0, \ldots, \mathcal{T}_2$ the input value to be the first value which is used by either g_1 or g_2. As a result, in step $\mathcal{T}_0$ the values at time instants $k = \{\nu;\ \nu + 4\}$ can be defined as input values. When in step $\mathcal{T}_1$ or $\mathcal{T}_2$, the input value is at time instant $k = \{\nu + 2;\ \nu + 3\}$. Unfortunately we cannot estimate the value for $u[\nu + 2]$ in $\mathcal{T}_1$, nor can we estimate $u[\nu + 3]$ in $\mathcal{T}_2$, because one half of the information has not been received, yet, (*i.e.*, missing information is located in the MSB in $\mathcal{T}_2$ and $\mathcal{T}_0$, respectively).

However, as all information on $u[\nu+1]$ (for which the output of g_1 was punctured) has been received in $\mathcal{T}_1$ we can estimate it. To do so we have to evaluate the MSB of the survivor state which is selected by the survivor path during the add-compare-select procedure within the VA. In $\mathcal{T}_2$, as already mentioned, selecting the survivor path allows a decision for two information bits (the MSB of the survivor *and* the input value) namely $u[\nu + 3]$ and $u[\nu + 4]$. At this point one has to evalutate the survivor state for the first information bit, and the survivor transition for the second one.

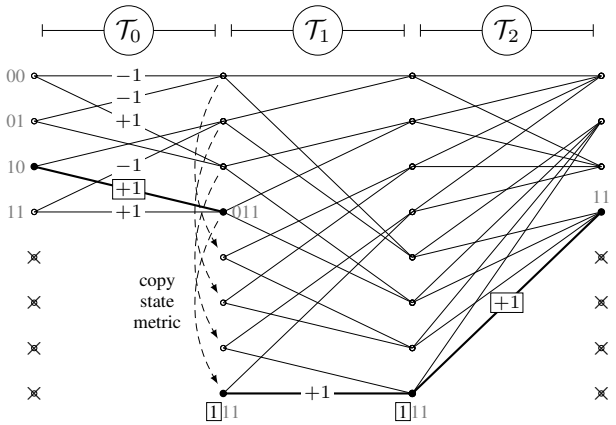

Fig. 9. Sample Trellis for Decoding

Fig. 9 illustrates where the information bits are located (boxed) by running the VA over one period of the trellis. As one can see the first two steps $\mathcal{T}_0$ have two transitions arriving at each state resulting in an estimation of a single bit per state. However, in the last step $\mathcal{T}_2$ the decision for a survivor gives an estimate on two bits. The path register of the VA has to consider the fact that now four bits have been estimated within three received symbols. The last step can be described as a state merging, where the split is performed in the first step, *e.g.* by copying the state metrics of the first four states into the last four states.

C. Increased Transmission Rate

In order to increase the transmission rate one can extend the size of the modulation alphabet and transmit n_u additional uncoded bits per modulation step, following the set-partitioning principle [1]. This TCM approach is well-understood and shall now be extended with puncturing as depicted in Fig. 1. By this, the total transmission rate is increased to (here, $R_\mathrm{c} \cdot n_\mathrm{c} = 1$)

$$R_\mathrm{PTCM} = R_\mathrm{p} + n_\mathrm{u}$$

with n_u and n_c denoting the number of uncoded and coded bits per symbol, respectively. In contrast to Ungerboeck's TCM, our proposed approach allows to adapt to an arbitrary transmission rate.

The resulting trellis is equal to that in Fig. 9 with 2^{n_u} parallel branches at each state. Each pair of parallel branches contain one uncoded bit information per trellis segment. However, three steps in the time-variant trellis contain four coded information bits. Thus, the total number of bits per trellis period is seven. We see, that the transmission of the coded and uncoded bits are not synchronized any longer.

V. Codes and Puncturing Schemes

As there is no analytical method known to the authors to find the optimal combination of channel (mother) code, puncturing and labeling for a given modulation scheme and constraint length, jointly, an exhaustive search was performed.

The search was carried out for convolutional codes with constraint length 5 (memory-4, *i.e.*, $\nu = 4$), natural labeling, and ASK modulation. The signal-to-noise power ratio $\frac{E_\mathrm{b}}{N_0}$ was between 6 and 12 dB and a transmission of 10^5 informations bits was performed.

In order to readuce the seach space, the puncturing schemes $P = [P_{ij}] \in \mathcal{P};\, i \in [1, 2];\, j \in [2, \cdots, \Omega]$, with the puncturing period Ω, are used to define the transmission rate and are constructed in such a way that the sum of the columns i follow the rule

$$\sum_{i=1}^{2} P_{ij} = \begin{cases} 2 & \text{if } j = 1 \\ 1 & \text{else.} \end{cases} \tag{2}$$

Hence, the rate of the puncturing scheme is $R_\mathrm{p} = \frac{\Omega+1}{\Omega}$.

The resulting generator polynomials in octal notation and puncturing schemes for the 16-state convolutional encoder are listed in Tab. I.

TABLE I
BEST MEMORY-4 ($\nu = 4$) CODES AND PUNCTURING SCHEMES FOR PUNCTURED CONVOLUTIONAL CODING WITH $R_\mathrm{c} = \frac{1}{2}$, $R_\mathrm{p} = \frac{\Omega+1}{\Omega}$.

R	$R_\mathrm{c} \cdot R_\mathrm{p}$	polynomials	puncturing scheme
4/3	2/3	$\left[26,\ 37\right]_8$	$\begin{bmatrix}1&0\\1&1\end{bmatrix}$
3/2	3/4	$\left[36,\ 23\right]_8$	$\begin{bmatrix}1&1&1\\1&0&0\end{bmatrix}$
8/5	4/5	$\left[34,\ 31\right]_8$	$\begin{bmatrix}1&0&1&0\\1&1&0&1\end{bmatrix}$
5/3	5/6	$\left[04,\ 37\right]_8$	$\begin{bmatrix}1&1&1&1&0\\1&0&0&0&1\end{bmatrix}$
12/7	6/7	$\left[34,\ 31\right]_8$	$\begin{bmatrix}1&0&1&0&1&0\\1&1&0&1&0&1\end{bmatrix}$

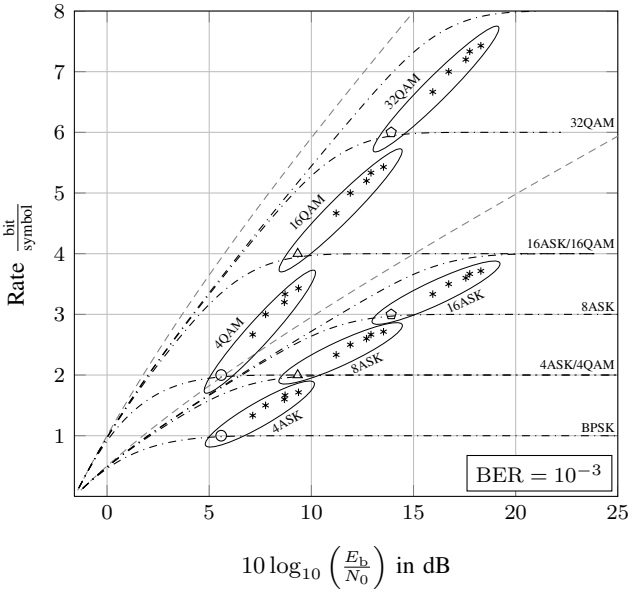

Fig. 10. Spectral efficiency vs. required $\frac{E_\mathrm{b}}{N_0}$ for a bit error rate of BER $= 10^{-3}$. Channel codes with 2^4 states. Shannon capacity constraint (dashed line, real-/complex-valued), Constellation capacity (dash-dotted line, ASK and QAM). Asterisk markers: proposed approach. Empty markers: Ungerboeck's TCM, $\mathcal{D} = 1$

VI. NUMERICAL RESULTS

Fig. 10 shows the simulation results for ASK modulation schemes. The 16-state channel codes are punctured from a rate $\frac{1}{2}$ mother code using the puncturing scheme as defindes in Table I. Higher transmission rates are achieved by additional uncoded bits and expansion of the constellation (*cf.*, Fig. 1), following the set partitioning principle.

Additionally, two consecutive ASK channel symbols are modulated to a two-dimensional quadrature-amplitude-modulation (QAM) symbol to further increase transmission rate without increasing the signal bandwidth.

The results clearly indicate that punctured TCM enables soft transitions between classical TCM rates (integers) by puncturing. By this means, the shape of the constellation constraint capacity can be closely approximated using punctured TCM.

VII. CONCLUSION

It has been shown that TCM can be extended by puncturing. We sketched the modifications necessary for the VA to properly work on the resulting time-variant trellises. Additionally, we conducted a computer search to optimize for the channel encoder and the puncturing scheme for ASK modulation. We further increased the transmission rate by appending uncoded information bits and thus enlarging the signal constellation as well as by implementing QAM transmission scheme using two subsequent ASK symbols.

The numerical simulation results clearly show that we can achieve a soft tradeoff between spectral and power efficiency easier and more flexible than by means of traditional TCM and multidimensional TCM.

REFERENCES

[1] G. Ungerboeck, "Channel coding with multilevel/phase signals," *IEEE Transactions on Information Theory*, vol. IT-28, no. 1, pp. 55 – 67, jan 1982.

[2] ——, "Trellis-coded modulation with redundant signal sets; part i: Introduction; part ii: State of the art," *Communications Magazine, IEEE*, vol. 25, no. 2, pp. 5 –21, February 1987.

[3] T. Hehn and J. B. Huber, "LDPC Codes and Convolutional Codes with Equal Structural Delay: A Comparison," *IEEE Transactions on Communications*, vol. 57, no. 6, pp. 1683–1692, June 2009. [Online]. Available: http://www.lit.lnt.de/papers/tr_com_2009_hehn.pdf

[4] E. Zehavi, "8-PSK Trellis Codes for a Rayleigh Channel," *IEEE Transactions on Communications*, vol. 40, no. 5, pp. 873 –884, may 1992.

[5] L.-F. Wei, "Trellis-coded modulation with multidimensional constellations," *IEEE Transactions on Information Theory*, vol. 33, no. 4, pp. 483 – 501, jul 1987.

[6] A. Viterbi, J. Wolf, E. Zehavi, and R. Padovani, "A pragmatic approach to trellis-coded modulation," *Communications Magazine, IEEE*, vol. 27, no. 7, pp. 11 –19, july 1989.

[7] T. Woerz and R. Schweikert, "Performance of punctured pragmatic codes," in *Global Telecommunications Conference, 1995. GLOBECOM '95., IEEE*, vol. 1, nov 1995, pp. 664 –669 vol.1.

[8] F. Schuh, A. Schenk, and J. Huber, "Reduced complexity Super-Trellis decoding for convolutionally encoded transmission over ISI-Channels," in *2013 International Conference on Computing, Networking and Communications, Signal Processing for Communications Symposium (ICNC'13 - SPC)*, San Diego, USA, Jan. 2013.

[9] ——, "Matched decoding for punctured convolutional encoded transmission over ISI-Channels," in *9th International ITG Conference on Systems, Communications and Coding 2013 (SCC'2013)*, Munich, Germany, Jan. 2013.